

Tribological Aspects Affecting Surface Durability of Tooth-Sum Altered Spur Gears: A Load Sharing Approach

Avil Allwyn Dsa^{1,*}, Joseph Gonsalvis²

¹Department of Mechanical Engineering, Don Bosco College of Engineering, Goa, India

²Research Advisor, Mechanical Engineering, St. Joseph Engineering College, Mangalore, India

Received 01 May 2022; received in revised form 01 June 2022; accepted 03 June 2022

DOI: <https://doi.org/10.46604/aiti.2023.9562>

Abstract

The performance of tooth-sum altered (ATS) gears is determined by the factors influenced by their profile geometry. This study aims to explore the influence of gear geometry modification on tribological aspects that affect surface wear in ATS spur gears. A computer code is developed to simulate surface wear numerically, using Archard's wear model, Greenwood-Williamson micro-asperity contact model, and Johnson's load-sharing approach. The outcomes of the study indicate that the low contact ratio ATS gears promote the formation of thick oil film owing to reduced specific sliding and increased speed. However, high contact ratio ATS gears create unfavorable operating conditions resulting in extreme boundary lubrication. The effectiveness of lubricant oil film in reducing wear in ATS gears is associated with its modified profile, sliding velocities, load bearing, operating temperature, and oil viscosity.

Keywords: altered tooth-sum gear, wear, lubrication, oil film, specific sliding

1. Introduction

The performance and surface durability of gear drives are greatly affected by the gear geometry, material properties, lubrication, and contact conditions. The gear profile is a macroscopic parameter, which affects almost all aspects of the performance of a gear drive. Hence, designers attempt profile modifications to improvise specific design features to fulfill the functional requirements of a gear pair. The tooth-sum altered (ATS) gearing [1-3], is a novel type of profile-shifted gearing system, which provides the flexibility of modifying the profile geometry by accommodating different tooth-sums on the same center distance.

Lubrication in ATS gears is influenced by profile modification that affects oil film thickness, sliding velocities, load-bearing, operating temperatures, oil viscosity, and consequently surface wear. A gear tooth contact is a non-conformal engagement under mixed elastohydrodynamic lubrication (EHL) [4], sharing the total load partially between the lubricating oil film and the participating surface asperities. The geometry-driven change in specific sliding and flash temperature at the tooth-contact interface causes variation in oil viscosity conditions, promoting mixed or boundary lubrication with partial metal-to-metal (asperities) surface contact. A favorable fluid film EHL regime can avoid such asperity contacts enhancing surface wear resistance. Surface roughness is also an important parameter that influences gear performance and surface wear. Under high load, the contact asperities undergo elastic and plastic deformation and cause an increase in friction, resulting in wear. The multi-parameter dependence of damage by wear makes it a complex problem that continues to be a common failure mode experienced by gear transmission systems.

* Corresponding author. E-mail address: avil.dsa@dbcegoa.ac.in

The objective of this work is to investigate the influence of tooth-sum alteration on lubrication, load bearing, coefficient of friction, and wear along different regions of the tooth flank. In this analysis, a surface wear model based on Archard's wear formulation [5] and Johnson's load-sharing concept [6] is used along with classical elastohydrodynamic lubrication theory [4] in predicting the tribological factors that influence surface damage in geometry-modified ATS gearing.

2. Literature Review

In recent years, a few researchers reported the benefits of gear profile modification by tooth-sum alteration of non-lubricated gears with smooth surfaces operating on a fixed center distance. Sachidananda et al. [1] showed it is possible to obtain either low, normal, or high contact ratio gear drives by altering the tooth-sum of a gear pair. They experimentally investigated the surface damage of non-lubricated spur gear contacts and confirmed the design benefits and flexibility of ATS gears. Sachidananda et al. [2] studied the effects of sliding velocity in ATS gears and concluded that negative tooth-sum alterations are better than standard or positive alterations in tooth-sum. Dsa and Gonsalvis [3] extended the tooth-sum alteration technique to asymmetric gears and studied surface wear in non-lubricated contacts.

Earlier, Johnson et al. [6] proposed a theoretical approach for studying highly loaded lubricated contacts by combining the established elastohydrodynamic theory and Greenwood and Williamson's [7] theory of rough random contact surfaces. They proposed the concept of the total load being shared between hydrodynamic pressure and surface asperity contacts. Gelinck and Schipper [8] used the load-sharing idea and developed a mixed lubrication model to obtain the Stribeck curves for line contact problems to predict transitions between lubrication regimes. Akbarzadeh and Khonsari [9] used the load-sharing approach to develop a model for predicting the performance of spur gears. They validated their model by comparing their predictions with published theoretical and experimental data.

Ebrahimi Serest and Akbarzadeh [10] presented a model for predicting the performance of helical gears, using the load-sharing concept for accounting for the contribution of surface roughness and the lubricant in bearing the applied load. Kimiaei and Akbarzadeh [11] used the load-sharing model to evaluate the performance of S_0 and S_{\pm} profile shifted gears. Simon [12-14] reported the results of his extensive work on full EHL analysis in different types of gears, investigating the influence of gear design, operating conditions, and lubricant on gear performance characteristics.

Over the years, researchers on surface wear of spur gears have mainly focused on developing prediction models, enhancing wear resistance by geometry modification and material properties. Archard's general wear equation [5] is a popular choice among researchers for wear prediction in gears having parameters with complex inter-dependency due to its simplicity and reasonably realistic estimate. Flodin and Andersson [15] proposed a numerical wear simulation model based on Archard's wear formulation employing the single-point contact observation technique. Prabhu Sekar and Sathishkumar [16] reported the possibility of enhancing the wear resistance in spur gears by profile shift.

In a study on the wear of asymmetric gears, Karpat and Ekwaro-Osire [17] found that tooth tip relief given could reduce induced dynamic load and wear depth. Brandão et al. [18] determined the roughness shape of the pinion tooth flank surface using a combined wear and surface contact fatigue damage model. Zhang et al. [19] experimentally investigated the wear and contact fatigue of modified involute gears under minimum lubrication, considering tooth wear evolution.

Ristivojevic et al. [20] studied the impact of geometric and operational parameters on surface wear and reported lesser wear on the addendum flank and higher wear on the dedendum. Ding and Kahraman [21] in their work on the interaction between gear dynamics and surface wear presented a set of simulations to demonstrate a two-way relationship between non-linear gear dynamics and surface wear. Reviewing the literature on ATS spur gears, the study of the tribological aspects affecting surface wear is identified as a research gap. In addition, Johnson's load-sharing concept which combines the classical EHL theory and micro-asperity contact model is identified as an efficient method to solve the mixed EHL problem with fairly good accuracy.

3. Gear Geometry Modification by Tooth-Sum Alteration

It is possible to accommodate different tooth-sums and gear ratios on a specified center distance. While the module m is a parameter that is critical for the magnitude of power transmitted, the gear ratio is important to maintain the required output speed. For a standard gear pair with reference tooth-sum z_s^r , the operating pressure angle ϕ_w and center distance c_w are the same as the standard pressure angle ϕ and center distance c_s^r . Keeping the center distance the same and altering the reference tooth-sum by a factor α to z_s^a , causes the operating pressure angle to change (refer to Fig. 1). Such gear pairs require a total profile shift coefficient X_s to be included for proper meshing [22]. Tooth topping of addendum radii of the mating gears by a factor: called tooth topping coefficient Y ensures adequate root clearance [23].

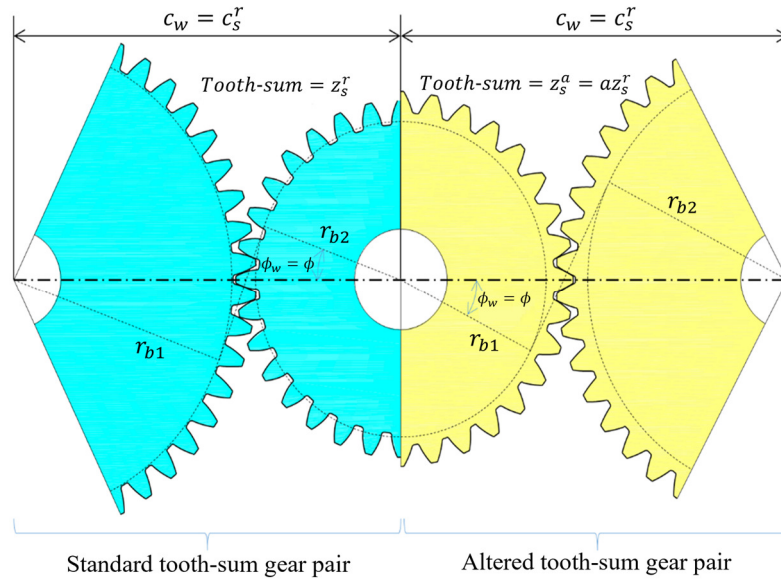


Fig. 1 Standard tooth-sum and altered tooth-sum gears

The ratio of profile shift coefficient x_1 on the driver to that of the total profile shift coefficient X_s for a gear pair is defined as the profile shift factor κ . If the tooth-sum [3] and the center distance of a reference gear pair are altered by a factor α and β respectively, it can be shown that:

$$\frac{\cos \phi_w}{\cos \phi} = \frac{\alpha}{\beta} \tag{1}$$

$$X_s = \frac{mZ_s^a (\text{inv} \phi_w - \text{inv} \phi) - B\alpha}{2m\beta \tan \phi} \tag{2}$$

$$Y = X_s + \frac{Z_s^r}{2} (\alpha - \beta) \tag{3}$$

$$\kappa = \frac{x_1}{X_s} \tag{4}$$

For a standard tooth-sum (STS) normal contact ratio (NCR) gear pair, $\alpha = \beta = 1$. For the ATS gear system, $0.96 < \alpha < 1.04$ and $\beta = 1$. For the S_{\pm} profile shifted system, $0.96 < \beta < 1.04$ and $\alpha = 1$. The performance characteristics of altered tooth-sum gears can be studied under a constant load or constant speed condition. The equation for tooth load on a pair of gears transmitting a power P at speed N under constant load can be expressed as:

$$F_t^r = F_t^a = \frac{P}{2\pi N r_b} \tag{5}$$

Altering the tooth-sum of a gear pair on a fixed center distance changes the radius of the base circles. To maintain constant load, the speed of the ATS gear pair should be changed. The equation for speed relation between the ATS and the STS gear pair is given by:

$$N^a = \frac{r_b^r}{r_b^a} \times \frac{F_t^r}{F_t^a} \times N^r \quad (6)$$

where N , F_t , and r_b represent the speed, normal load, and radius of the base circles, respectively. The superscripts r and a represent reference gear and altered gear pairs, respectively. For a constant load using $F_t^r = F_t^a$ Eq. (6) reduces to:

$$N^a = \frac{r_b^r}{r_b^a} \times N^r \quad (7)$$

4. Load Sharing and Friction Coefficient in ATS Gears under Boundary Lubrication

In ATS gears operating under a boundary lubrication regime, the total load transmitted is assumed to be shared between the oil film and the contacting asperities [6]. The dynamic load f_{dx} shared by a tooth pair at any arbitrary location is equal to the sum of the load carried by the asperities f_c and oil film f_{hy} , and it can be expressed as:

$$f_{dx} = f_{hy} + f_c \quad (8)$$

Dividing throughout by f_{dx} Eq. (8) can be written as:

$$\frac{f_{hy}}{f_{dx}} + \frac{f_c}{f_{dx}} = 1 \quad (9)$$

Defining $1/\gamma_1$ and $1/\gamma_2$ as load sharing factors for the hydrodynamic part and asperities contact part respectively, Eq. (9) can be written as:

$$\frac{1}{\gamma_1} + \frac{1}{\gamma_2} = 1 \quad (10)$$

Similarly, the total friction force μf_{dx} at any location is the sum of the oil film friction force $f_{\mu hy}$ and asperities contact friction force $\mu_c f_c$. Mathematically:

$$\mu f_{dx} = f_{\mu hy} + \mu_c f_c \quad (11)$$

Dividing Eq. (11) throughout by f_{dx} and using the definition of $1/\gamma_2$ from Eq. (10), the total friction coefficient μ is given by:

$$\mu = \frac{f_{\mu hy}}{f_{dx}} + \frac{\mu_c}{\gamma_2} \quad (12)$$

From Newton's law of viscosity, the hydrodynamic friction force $f_{\mu hy}$ per unit, face width is given by:

$$f_{\mu hy} = 2a\eta \frac{v_{r1} - v_{r2}}{h_c} \quad (13)$$

where a is the Hertzian half-width of contact, η is the dynamic viscosity at contact pressure, v_r is the rolling velocity of gears and h_c is the oil film thickness. Using simplified Roeland's equation, lubricant viscosity at any contact pressure and temperature can be found.

$$\eta = \eta_{\infty} \times e^{2.303G_0(1+p/c)^{z_i}/(1+t/135)^{S_0}} \quad (14)$$

where z_i is called the viscosity pressure index assumed to be 0.6 for mineral oils, $\eta_{\infty} = 6.315 \times 10^{-5} Pa \cdot sec$, and the value of $c = 196 Mpa$. G_0 and S_0 are dimensionless numbers for lubricant viscosity grade and slope. The Hertzian half-width of contact is given by:

$$a = \sqrt{\frac{8f_{dx}\rho'}{\pi E'}} \quad (15)$$

$$\rho' = \frac{\rho_1\rho_2}{\rho_1 + \rho_2} \quad (16)$$

$$\frac{2}{E'} = \frac{1-\nu_1^2}{E_1} + \frac{1-\nu_2^2}{E_2} \quad (17)$$

where, using the modulus of elasticity E and the poisons ratio ν , the equivalent modulus of elasticity E' is defined using Eq. (17). Using the radius of curvature ρ at any contact location, the equivalent radius of curvature ρ' is defined using Eq. (16).

5. Flash Temperature and Oil Film Thickness

The operating condition at the contact interface depends upon gear geometry, loading conditions, and lubricant properties as the point of contact glides along the pressure line. The sliding motion in a gear contact increases the temperature of its contact interface, which can break down the lubricating oil film. Flash temperature is defined as the instantaneous rise in surface temperature when contact between gear teeth occurs. Blok's flash temperature equation formulated by AGMA is given as:

$$T_f = \frac{0.8\mu x_{dl}F}{B_m a^{0.5}} |(v_{r1})^{0.5} - (v_{r2})^{0.5}| \quad (18)$$

Temperature changes the oil viscosity, consequently affecting oil film formation. The central oil film thickness calculation is based on Moe's equation [4]. The following dimensionless numbers are used in defining Moe's numbers.

$$W = \frac{f_{dx}}{E'\rho'} \quad (19)$$

$$U_{\Sigma} = \frac{\eta_0(v_{r1} + v_{r2})}{E'\rho'} \quad (20)$$

$$G = \alpha_{ehl}E' \quad (21)$$

where W is the dimensionless load parameter, U_{Σ} is the dimensionless speed parameter, α_{ehl} is called the Barus pressure viscosity coefficient. The dimensionless Moe's numbers are defined as:

$$H_c = \frac{h_c}{\rho'} U_{\Sigma}^{-1/2} \quad (22)$$

$$M = W U_{\Sigma}^{-1/2} \quad (23)$$

$$L = G U_{\Sigma}^{1/4} \quad (24)$$

Moe's equation for central oil film thickness modified by Gelinck and Schipper [8] using Johnson's load-sharing method is given as:

$$H_c = \left[\gamma_1^{s/2} \left(H_{ri}^{7/3} + \gamma_1^{-14/15} H_{ei}^{7/3} \right)^{3s/7} + \gamma_1^{-s/2} \left(H_{rp}^{-7/2} + H_{ep}^{-7/2} \right)^{-2s/7} \right]^{1/s} \gamma_1^{1/2} \quad (25)$$

$$H_{ri} = 3M^{-1} \quad (26)$$

$$H_{ei} = 2.621M^{-1/5} \quad (27)$$

$$H_{rp} = 1.287L^{2/3} \quad (28)$$

$$H_{ep} = 1.311 \left(M^{-1/8} L^{3/4} \right) \quad (29)$$

$$s = \frac{1}{5} \left(7 + 8e^{-\frac{2\gamma_1^{-2/5} H_{ei}}{H_{ri}}} \right) \quad (30)$$

The subscripts ri , rp , ei , and ep denote rigid-iso-viscous; rigid-piezoviscous; elastic-iso-viscous, and elastic-piezoviscous, respectively. The type of lubrication regime is determined based on the value of the roughness parameter given by:

$$\Lambda = \frac{h_c}{\sigma_{rms}} \quad (31)$$

The value of $\Lambda > 3$ represents full oil film, $1 < \Lambda < 3$ represents mixed lubrication regime, and $\Lambda < 1$ represents boundary lubrication. According to Greenwood-Tripp's asperity contact model [24], the average contact pressure can be expressed as:

$$p_c = \frac{8\sqrt{2}}{15} \pi (n' \beta' \sigma_{rms})^2 \sqrt{\frac{\sigma_{rms}}{\beta'} E' F_{5/2}} \frac{h_c - d_d}{\sigma_{rms}} \quad (32)$$

where n' is the density, β' is the radius of curvature of the asperities, and σ_{rms} is the composite root mean square surface finish.

The $F_{5/2}$ function can be approximated by:

$$F_{5/2}(H_\sigma) = \begin{cases} 4.4068 \times 10^{-5} (4 - H_\sigma)^{6.804} & \text{for } H_\sigma \leq 4 \\ 0 & \text{for } H_\sigma > 4 \end{cases} \quad (33)$$

Applying Johnson's concept of load sharing, Gelinck and Schipper have shown that central pressure is a good quantity to characterize the pressure distribution of rough line contact. Mathematically:

$$p_c = \frac{1}{\gamma_2} \sigma_{fc} \left\{ 1 + \left[1.558 \left(\gamma_2 n' \rho' \sqrt{\beta' \rho'} \right)^{0.0337} \left(\frac{\sigma_{rms}}{\rho'} \right)^{-0.442} W^{0.4757} \right]^{-1.7} \right\}^{-0.5882} \quad (34)$$

$$\sigma_{fc} = \sqrt{\frac{f_{dx} E'}{2\pi \rho'}} \quad (35)$$

where Eq. (35) gives the variation of contact stress σ_{fc} along the line of action.

6. Static and Dynamic Load Factors

Evaluation of static and dynamic loading patterns for ATS gears with different values of tooth-sum alteration factors α is essential to identify the effect of gear geometry modification on various performance parameters. If λ_x is the mesh stiffness [25] at any arbitrary contact location for tooth load intensity per unit face width f_x , then static load factor χ_l is defined as the ratio of location-based mesh stiffness to that of equivalent mesh stiffness λ_{eq} . It can be expressed as:

$$x_l = \frac{\lambda_x}{\lambda_{eq}} \tag{36}$$

A gear pair in the mesh can be modeled as a single-degree-of-freedom spring-mass damper system subjected to forced vibration [26] to evaluate dynamic load factors for ATS gears. The one DOF model considers the influence of mesh stiffness, damping forces, friction forces, and the static transmission error at the mesh interface and is expressed as a time-varying function. The gear pairs are assumed to be of unit face width and free of tooth profile errors. The differential equations of motion for this system can be expressed in the form:

$$m_{eq}\ddot{x}_r + c_{eq}\dot{x}_r + k_{eq}x_r = F \tag{37}$$

$$m_{eq} = \frac{m_{e1}m_{e2}}{m_{e1} + m_{e2}} \tag{38}$$

$$k_{eq} = \frac{m_{e2} \sum_{i=1}^n \lambda_i (1 \pm \mu\theta_{1i}) + m_{e1} \sum_{i=1}^n \lambda_i (1 \pm \mu\theta_{2i})}{m_{e1} + m_{e2}} \tag{39}$$

$$c_{eq} = 2\xi\sqrt{m_{eq}k_{eq}} \tag{40}$$

where $m_e = 1/2m_g$ is the effective mass of the pinion and the gear, F is the static load, and θ is the roll angle. Equivalent mass, stiffness, and damping coefficient are denoted by m_{eq} , c_{eq} , and k_{eq} . The solution of the differential equation provides relative displacement x_r at the contact interface, which is used to evaluate dynamic loads f_{dx} and dynamic load factors x_{dl} .

$$f_{dx} = x_r \lambda_{eq} \tag{41}$$

$$x_{dl} = \frac{f_{dx}}{F} \tag{42}$$

7. Surface Wear in Gears

Surface wear in gears is a material attrition phenomenon from the contacting surface subjected to partial sliding and rolling action. Flodin and Andersson [15] employed a single-point observation-based gear contact methodology in conjunction with Archard’s wear formulation to evaluate surface wear in dry and boundary-lubricated sliding surfaces of a meshing gear pair. The accumulated wear h_{xn} at any location after n cycles is given as:

$$h_{x,n} = h_{x,n-1} + 2k_w \sigma_{fc} a \frac{v_{r1} - v_{r2}}{v_{r1}} \tag{43}$$

where v_r is the sliding velocity and σ_{fc} is the contact pressure. The term within the parenthesis $[(v_{r1} - v_{r2})/v_{r1}]$ represents specific sliding V_{ss} which is the ratio of relative sliding per unit rolling.

Using the load factor γ_2 for load taken up by the asperities and $\sigma_{fc} a = 2f_{dx}/\pi$ [22], Eq. (43) can be rewritten as:

$$\begin{cases} h_{x,n} = h_{x,n-1} + 4k_w \frac{f_{dx}}{\gamma_2 \pi} V_{ss} \\ h_{x,n} = h_{x,n-1} + 4 \frac{F}{\pi} \times k_w \frac{x_{dl} V_{ss}}{\gamma_2} \end{cases} \tag{44}$$

where F is the load transmitted per unit face width, h_{xn} is the accumulated wear after n cycles, f_{dx} is the dynamic load per unit face width, x_{dl} is the dynamic load factor, a is the semi-contact width of the elliptical contact and k_w is the wear coefficient. The total profile error ε_x , dynamic load f_{dx} , and load factor x_{dl} at any location after n cycles is given by:

$$\varepsilon_{xn} = h_{xn}^1 + h_{xn}^2 \quad (45)$$

$$f_{dx} = \lambda_x (x_r - \varepsilon_x) \quad (46)$$

$$x_{dl} = \frac{f_{dx}}{F} \quad (47)$$

8. Gear Pitting Life

A model for predicting the pitting fatigue life of rolling bearings, proposed by Lundberg and Palmgren [27] was extended by Coy et al. [28] to spur gears because of the similarities in their fatigue failure mechanism. The tooth profile and the contact zone along the pressure line are divided into finite intervals to predict gear life based on dynamic loads. The use of intervals allows the model to account for load and curvature sums varying with contact position. Life estimation of each interval is used to determine complete gear tooth life using probability and statistics methods.

$$L = \left(\sum_{x=1}^n L_x^e \right)^{-1/e} \times b^{-0.4} \quad (48)$$

where e is the Weibull exponent whose value is taken to be 2.5 for steels, b is the face width of the gear and L_x is the life for a 90% probability of survival of a single tooth subjected to a load F per unit face width is given by:

$$L_x = \left(B \frac{\gamma_2}{x_{dl} F} \right)^{4.3} (\rho')^5 \left(\frac{1}{l} \right)^{0.4} \quad (49)$$

where constant material B is taken as 1.32×10^8 for SI units, l is the involute curve length and ρ' is the equivalent radius of curvature.

9. Investigation Methodology

A reference gear pair of module $m = 3 \text{ mm}$, tooth-sum $z_s^r = 100$, and pressure angle $\phi = 20^\circ$ transmitting 10 kW power @800 rpm between a center distance $c_w = 150 \text{ mm}$ is altered with tooth-sum alteration factor $0.96 \leq \alpha \leq 1.04$ for this case study. The calculation of the ATS geometry modification parameters as described in Section 3 and Eqs. (1)-(3) are presented in Table 1. The total shift X_s is shared between the pinion and the gear using the profile shift factor $0.25 \leq \kappa \leq 0.75$ given by Eq. (4).

Table 1 ATS gear geometrical parameters

Standard gear of $m = 3 \text{ mm}$, $z_s^r = 100$, $\phi = 20^\circ$, and $B = 0.2 \text{ mm}$				
α	$z_s^a = \alpha z_s^r$	$\phi_w = \cos^{-1} \left(\frac{\alpha}{\beta} \times \cos \phi \right)$	$X_s = \frac{m\beta Z_s^a (\text{inv}\phi_w - \text{inv}\phi) - B\alpha}{2m\beta \tan \phi}$	$Y = X_s + \frac{Z_s^r}{2} (\alpha - \beta)$
0.96 (ATS)	96	0.4461	2.18748	0.1875
0.98 (ATS)	98	0.4004	0.9806	-0.0194
1 (STS)	100	0.349	0	0
1.02 (ATS)	102	0.2892	-1.0154	-0.0154
1.04 (ATS)	104	0.2135	-1.7538	0.2461

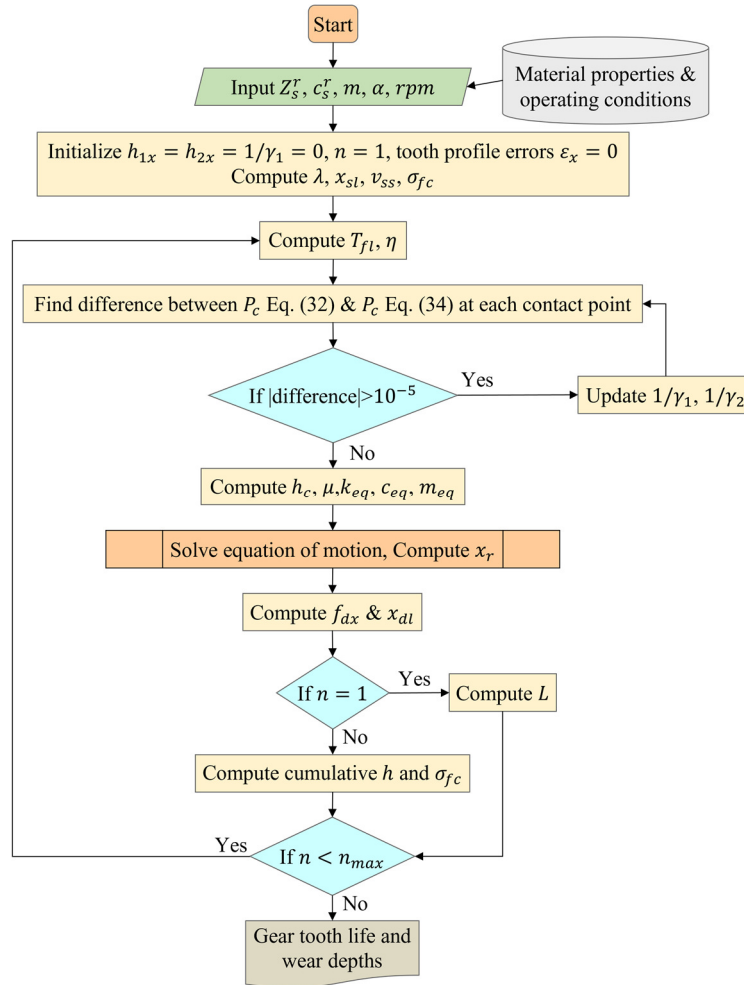


Fig. 2 Numerical simulation flow chart

Altering the tooth-sum of a reference gear pair changes the radii of the base circles. The pressure angles, profile shift factor, and tooth topping collectively decide the geometry of the ATS gears. The radius of the addendum circle r_a is calculated using the relation:

$$\begin{cases} r_{a1} = r_1 + (\kappa X_s + Y + 1)m \\ r_{a2} = r_2 + [(1 - \kappa X_s) + Y + 1]m \end{cases} \quad (50)$$

The tooth load on ATS and STS gears transmitting 10 kW power @800 rpm are found using Eq. (5). The speed calculated using Eq. (7) to evaluate the performance of ATS gear under constant load is tabulated in Table 2. The material properties, surface, and operating conditions used in the simulation are given in Table 3.

Table 2 Load and speed data

Standard gear of $m = 3 \text{ mm}$, $z_s^r = 100$, $\phi = 20^\circ$, and $GR = 1:1$					
α	$z_s^a = \alpha z_s^r$	$z_1 = z_2 = z$	$r_b = (mz/2)\cos\phi$	$F_t^r = F_t^a = \frac{P}{2\pi N r_b}$	$N^a = \frac{r_b^r}{r_b^a} \times N^r$
0.96 (ATS)	96	48	67.659 mm	1694 N	833 rpm
0.98 (ATS)	98	49	69.069 mm	1694 N	816 rpm
1 (STS)	100	50	70.479 mm	1694 N	800 rpm
1.02 (ATS)	102	51	71.88 mm	1694 N	784 rpm
1.04 (ATS)	104	52	73.298 mm	1694 N	769 rpm

The procedure to find dynamic load factors and load sharing factors are iterative. The length of the contact path is divided into a finite number of intervals. The simulation procedure begins with selecting a trial value of load sharing factor for oil film

$1/\gamma_1$, and the oil film thickness is evaluated using Eq. (25). Using the trial value of $1/\gamma_2$ and oil film thickness h_c , Eqs. (32) and (34) are equated for equivalence within a degree of acceptable error. The process is iterated for the point of contact with different trial values of $1/\gamma_1$ until convergence is achieved. Using Eqs. (10) and (12), the load sharing factor for asperities $1/\gamma_2$ and the coefficient of friction can be obtained. The relative displacement at the mesh interface is obtained by solving one DOF dynamic model equation (refer to Eq. (37)).

Table 3 Material properties and operating conditions

Density of steel	7700 kg/m ³	Load per unit face width, F	1.7×10^5 N
Young's modulus, E	206 Gpa	The radius of curvature of asperities, β'	10 μ m
Wear coefficient, k_w	2×10^{-16} m ² N ⁻¹	The density of asperities, n'	1.25×10^{10} /m ²
Damping factor, ξ	0.25	Pressure viscosity coefficient, α_{ehl}	2.28×10^{-8} Pa ⁻¹
Dyn oil viscosity, η_0	0.05 Pa-s	Pressure viscosity index, z_i	0.6
Composite surface roughness, σ_{rms}	0.4 μ m	Thermal contact coefficient, B_m	13.6×10^6 N/m. s ^{0.5} K
The friction width of pinion and gear, b	10 mm	The friction coefficient for asperities, μ_c	0.1

Archard's wear model modified by Flodin and Andersson [15] for mild wear is employed to estimate wear rates and update dynamic load effects on oil film thickness, load sharing factors, and coefficient of friction. The Lundberg-Palmgren model is used for estimating fatigue pitting life. The flow chart of the computer code used for the numerical simulation of gear performance is shown in Fig. 2. The computation time required for one million cycles is approximately 3 hours for a pair of gears on a Pentium Octa-core 3.3 GHz machine.

10. Results and Discussion

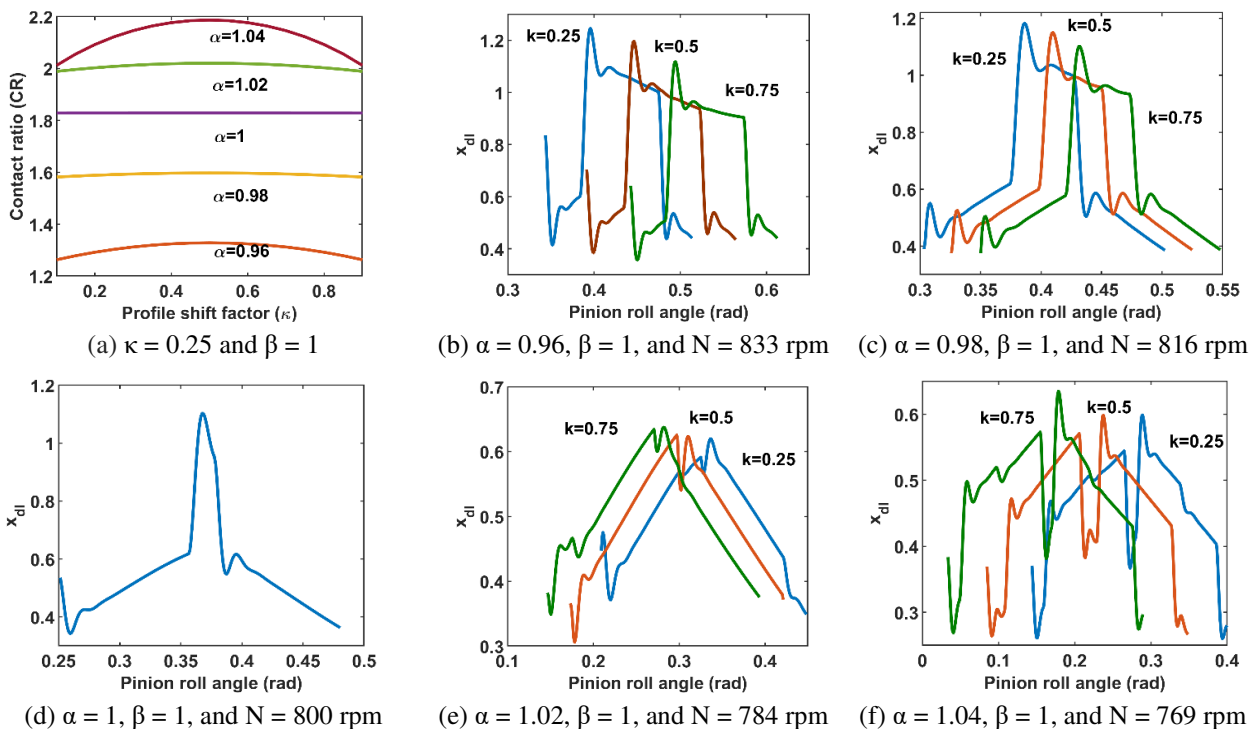


Fig. 3 Contact ratio and dynamic load factors

Gear contact mechanics is quite a complex phenomenon influenced by many parameters. Gear geometry is one of the primary parameters that when altered affects many tribological aspects influencing durability and life. ATS gears are addendum modified, tooth topped, profile shifted system operating on a fixed center distance. Contact ratio (CR) is a geometric parameter that indicates the influence of gear geometry on its load-sharing pattern. One way to increase the contact ratio of a

gear pair operating between a given center distance is to increase its tooth-sum. In ATS gears, increasing the tooth-sum decreases the overall tooth height which increases the mesh stiffness affecting dynamic load factors due to tooth topping. The preliminary investigation of ATS gears based on contact ratio reveals the possibility of achieving high contact ratio (HCR) ATS gears with positive tooth alterations ($\alpha > 1$), and low contact ratio (LCR) ATS gears with negative tooth alterations ($\alpha < 1$), all pairs running on the same center distance (refer to Fig. 3(a)).

Speed and contact ratio affect dynamic load factors in STS as well as ATS gears. Plots of dynamic load factors of NCR STS gears and LCR ATS gears for profile shift factors $0.25 < \kappa < 0.75$ show one region of single tooth contact and two regions of double tooth contact (refer to Figs. 3(b)-(d)). Larger zones of single tooth contact represent a lower contact ratio, and reducing the roll angle of single tooth contact shows improvement in the contact ratio. Plots of dynamic load factors of HCR ATS gears with $CR > 2$, show three regions of triple teeth contact and two regions of double tooth contact, indicating an improvement in the load-bearing capacity (refer to Figs. 3(e)-(f)). Spikes are observed at the transition zones between double to single tooth contact and triple to double tooth contact. As the speed increases, the dynamic load as a function of contact position differs appreciably from the static load. Dynamic load in a gear system decreases with an increase in contact ratio at any given speed because of the narrow single or triple contact zone, which passes quickly, leaving no time for the system to respond.

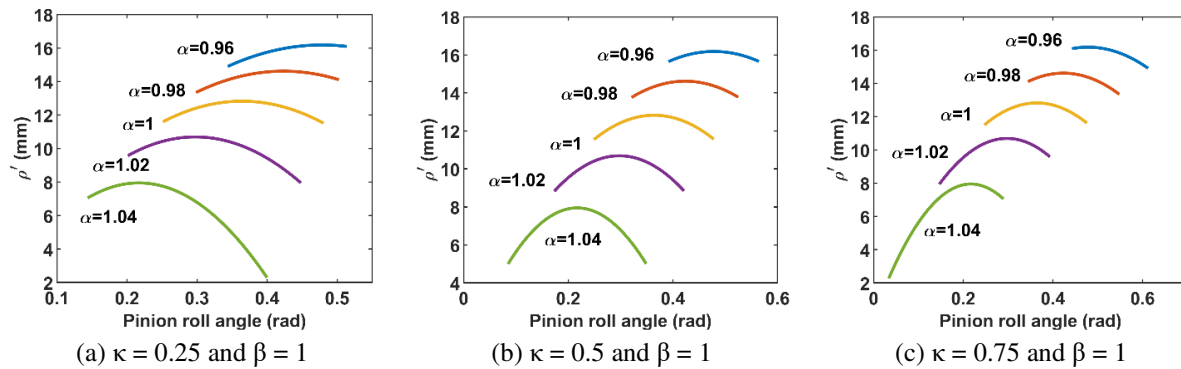


Fig. 4 Effective radius of curvature for ATS gears $0.96 < \alpha < 1.04$

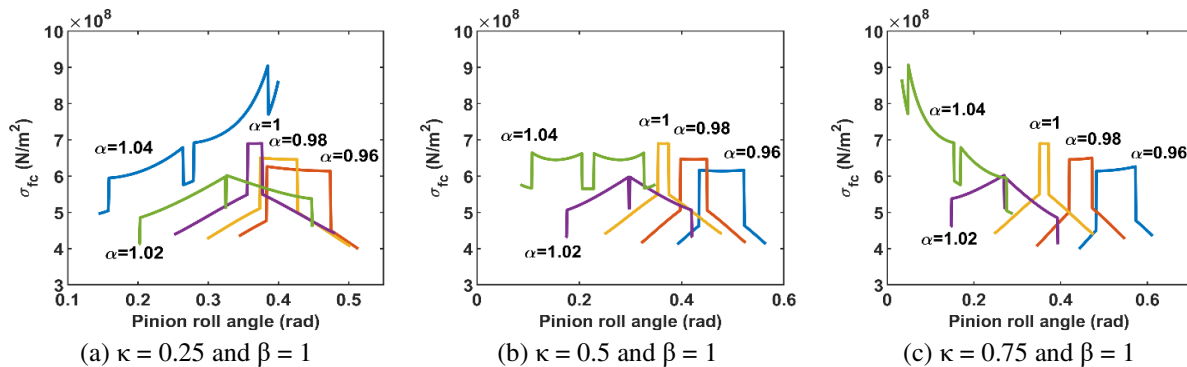


Fig. 5 Contact stresses for ATS gears $0.96 < \alpha < 1.04$

ATS gear geometry modification influences dynamic loads, contact pressure, and sliding velocities, consequently affecting flash temperature, oil viscosity, and film thickness. For a given load, the contact stress in ATS gears solely depends on the effective radius of curvature of the tooth (refer to Fig. 4). The effective radius of curvature is larger in LCR ATS and smaller in HCR ATS than the NCR STS. The effect of profile shift factor $0.5 < \kappa$ is to reduce the effective radius of curvature of the point of engagement in LCR ATS gears and increase the same at the point of disengagement in HCR ATS gears. Profile shift factor $\kappa > 0.5$ reduces the effective radius of curvature of the point of disengagement in LCR ATS gears and increases the same at the point of engagement in HCR ATS gears. Consequently, LCR ATS gears have lower magnitudes of contact

stresses than NCR STS, but the variation from single to double tooth contact region is significant. In HCR ATS, the highest magnitude of contact stress is comparable with LCR ATS, and the variation from two to three teeth contact region is comparatively less (refer to Fig. 5).

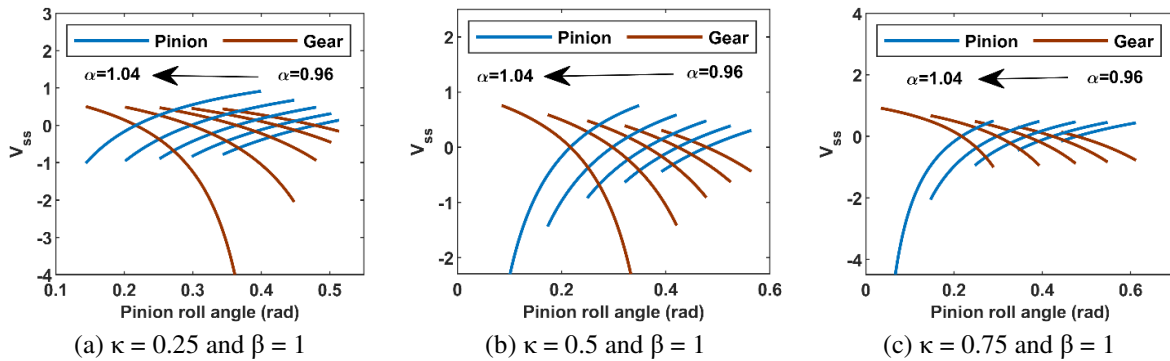


Fig. 6 Specific sliding in ATS gears $0.96 < \alpha < 1.04$

Specific sliding, contact stresses, and dynamic load factors are important indicators useful in contact wear analysis to quantify and compare damage by failure-promoting mechanisms such as fatigue, pitting, and abrasion in ATS gears. NCR STS and LCR ATS gears exhibit lower sliding velocities but higher dynamic loads. In contrast, HCR ATS gears show higher sliding speeds but lower dynamic loads (refer to Figs. 3(b)-(f) and Fig. 6). In any ATS gear pair, profile shift factor $\kappa < 0.5$ increases the specific sliding at the start point of mesh in LCR ATS and the endpoint in HCR ATS. On the contrary, the ATS gear pair with profile shift factor $\kappa > 0.5$ increases the specific sliding at the endpoint in LCR ATS and the start point of mesh in HCR ATS. For all the values of tooth-sum alteration factor α , the flash temperatures obtained using Blok’s contact temperature expression show the least value at the pitch point and gradually increase towards the beginning and end of the tooth mesh (refer to Fig. 7). Flash temperatures are affected by speed, dynamic load factors, and coefficient of friction. Specific sliding reduction or increase is associated with the speed and radius of curvature that influences flash temperature.

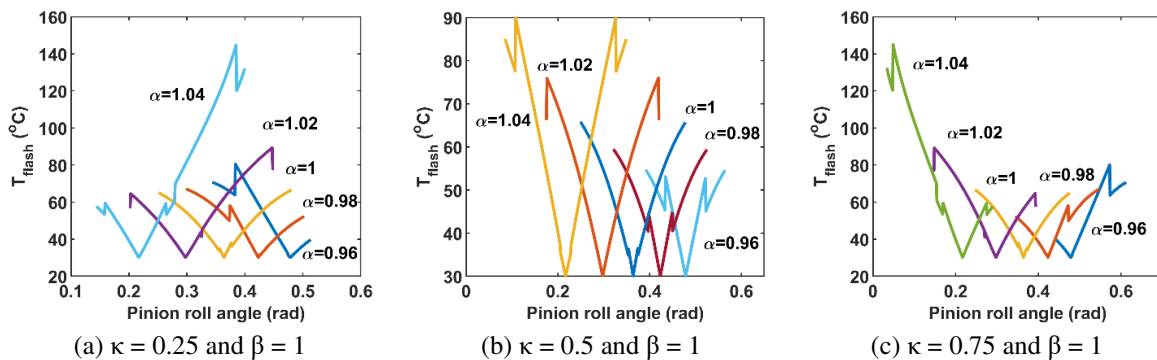


Fig. 7 Flash temperature for ATS gears $0.96 < \alpha < 1.04$

ATS gears with profile shift factor $\kappa = 0.5$, irrespective of the value of their tooth-sum alteration factor α , have symmetric temperature distribution about the pitch point. Flash Temperature distribution about the pitch point in LCR and HCR ATS gears operating with profile shift factor, $\kappa = 0.5$ can be compared with NCR STS gears under constant load conditions. Reduced relative sliding and higher oil film thickness due to higher speeds cause a reduction in the coefficient of friction, which helps reduce the flash temperature in ATS LCR gears. Higher relative sliding velocity and reduced oil film thickness due to lower operational speeds increase the coefficient of friction and flash temperature in HCR ATS gears. In any ATS gear pair, varying the profile shift factor κ alters the temperature distribution about the pitch point.

In an LCR ATS gear pair, the relative sliding velocity increases at the point of engagement and disengagement for gears operating with profile shift factor $\kappa < 0.5$ and $\kappa > 0.5$, respectively. In an HCR ATS gear pair, the relative sliding velocity increases at the point of disengagement and engagement for gears operating with profile shift factor $\kappa < 0.5$ and $\kappa > 0.5$,

respectively. Increased relative sliding and comparatively larger dynamic loads due to opposing friction forces consequently increase flash temperature and reduce dynamic viscosity and oil film thickness when operating the gears under constant load and speed conditions. Even though HCR ATS gears have lower dynamic loads, larger sliding velocities result in higher magnitudes of flash temperatures than LCR ATS gears.

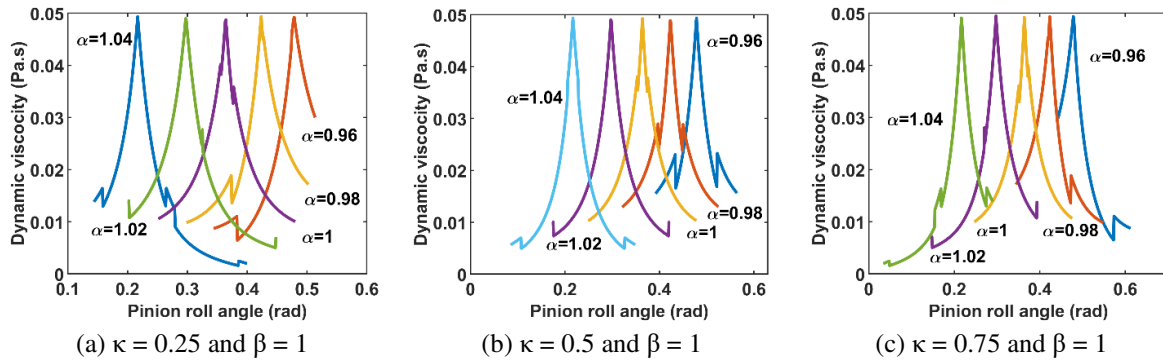


Fig. 8 Dynamic viscosity ATS gears $0.96 < \alpha < 1.04$

The dynamic viscosity for LCR and HCR ATS gears with profile shift factor $0.25 < \kappa < 0.75$ are plotted using Roeland's temperature-pressure-viscosity relation shows the largest magnitude at the pitch point and starts reducing on either side of it (refer to Eq. (14), Fig. 8). Dynamic viscosity is lower at the locations of higher flash temperatures and pressures with the least magnitudes at the beginning and end of contact in HCR ATS gears. Lower flash temperatures and pressures result in a comparatively smaller range of variation in viscosity in ATS LCR gears. Even though the HCR ATS gears have a higher load-carrying capacity than their LCR ATS counterparts, for a given load, a drop in viscosity results in reduced oil film thickness (refer to Fig. 9).

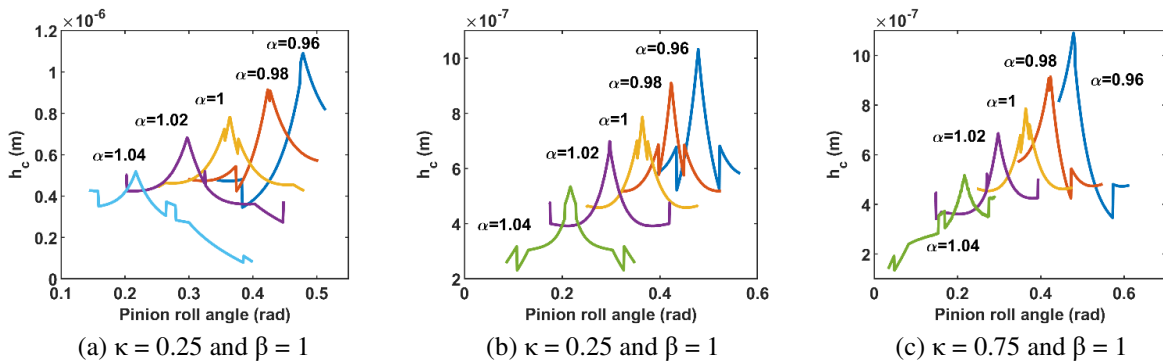


Fig. 9 Oil film thickness ATS gears $0.96 < \alpha < 1.04$

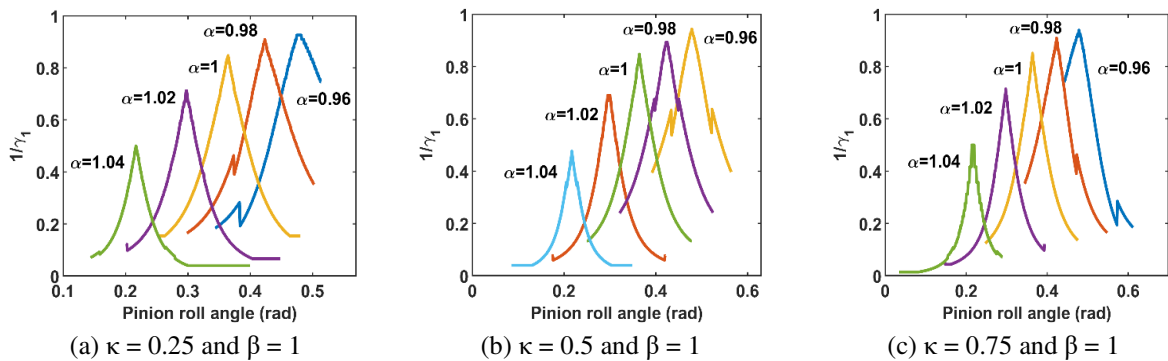


Fig. 10 Load on oil film ATS gears $0.96 < \alpha < 1.04$

The reduction in oil film thickness causes the asperities to take a considerable portion of the load and vice versa, especially at the start point and the endpoint of contact (refer to Fig. 10). The load sharing graphs indicate a maximum of 60% load taken up by the oil film at the pitch point, and the same reduces to below 10% at the extreme ends of mesh for HCR ATS gears. A more

significant portion of the load taken up by asperities due to thin oil film can cause the HCR ATS gears to operate under extreme boundary lubrication conditions. Improved oil film thickness in LCR ATS gears share a higher load of above 90% at the pitch point, reducing to 50% at the extreme ends of the mesh. The reduced oil film thickness causes a higher load share on the asperities resulting in a higher coefficient of friction in HCR ATS gears and vice versa in LCR ATS gears (refer to Fig. 11).

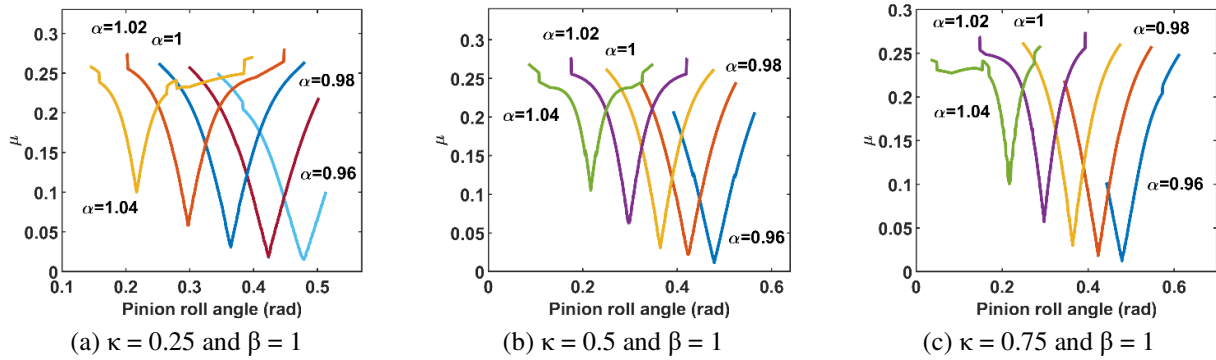


Fig. 11 coefficient of friction ATS gears $0.96 < \alpha < 1.04$

The higher the percentage of load taken by the oil film, the lesser the load on the surface asperities, and the better will be the life of the gear (refer to Fig. 12). Hence, LCR ATS gears will have a better life under the given loading conditions due to relatively thicker oil film formation than HCR ATS gears. The oil film thickness can be maintained by changing the oil or the operating speeds. Under the given operating conditions, the service life of HCR ATS can be improved by using oil of higher viscosity. However, using higher viscosity oil to avoid surface damage may increase power loss. Speed, dynamic load, and specific sliding are the important factors influencing the formation of the oil film and consequently the load distribution and wear. Plots of accumulated wear in NCR ATS gears operating under constant load and speed conditions are presented in Fig. 13.

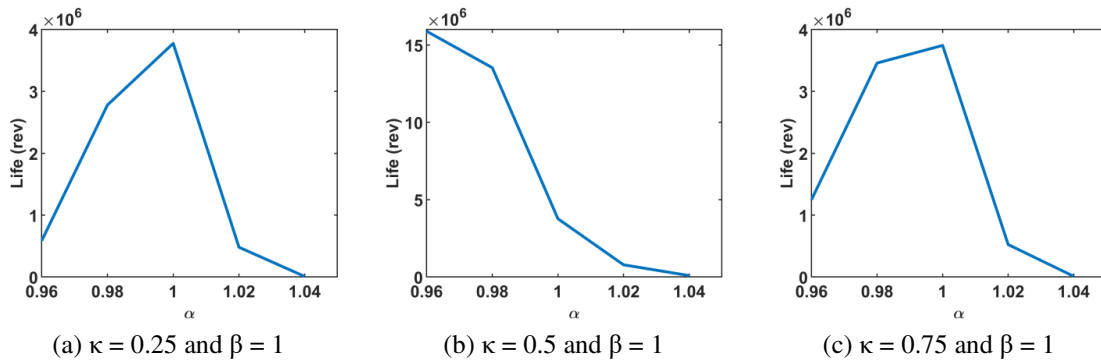


Fig. 12 Tooth life estimate ATS gears $0.96 < \alpha < 1.04$

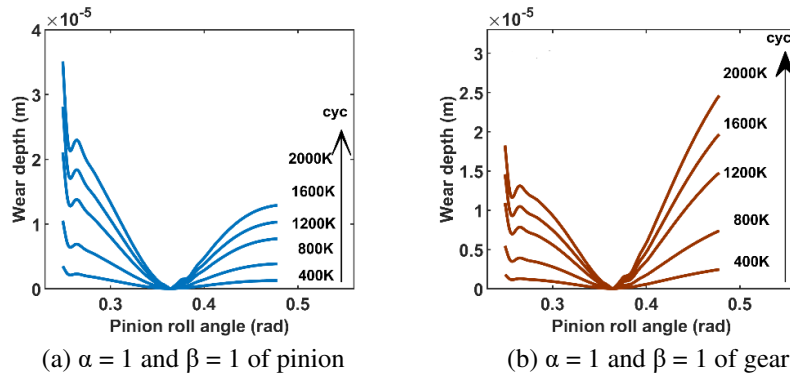


Fig. 13 Wear plots STS gears $\alpha = 1$ for 2×10^6 cycles

Varying the profile shift factor κ of any LCR ATS gear pair alters the mesh zone about its pitch point. The Profile shift factor $\kappa < 0.5$ makes the drive approach dominant by reducing the length of the path of recess and increasing the length of the approach. The specific sliding increases at the point of engagement and decreases at disengagement for both the pinion and the

gear, compared with the ATS LCR gears with profile shift factor, $\kappa = 0.5$. Increased specific sliding and relatively larger dynamic loads due to opposing friction forces eventually raise the flash temperature reducing dynamic viscosity and oil film thickness. Consequently, there is a proportional increase in wear on the pinion than on the gear in the approach engagement region and vice versa in the recess engagement region (refer to Figs. 14(a)-(b) & Figs. 15(a)-(b)), while the gears are operating under constant load condition.

For profile shift factor $\kappa = 0.5$, the LCR ATS gears, irrespective of their tooth-sum alteration factor α , attain equal approach-recess action. Accumulated wear is comparatively lesser than NCR STS gears (refer to Figs. 14(c)-(d) and Figs. 15(c)-(d)). Reduced specific sliding and improved oil film thickness due to increased speed help reduce wear rates in ATS LCR gears. Alternatively, increasing the profile shift factor $\kappa > 0.5$ decreases the path of approach and proportionately increases the path of recess, making the drive recess dominant. The specific sliding decreases at the engagement point and increases at disengagement for both pinion and gear. Higher specific sliding on the gear than on the pinion at the point of disengagement causes an increase in flash temperature, consequently reducing dynamic viscosity and oil film thickness. This leads to a relative increase in wear on gear than on the pinion in the recess engagement region and vice versa (refer to Figs. 14(e)-(f) and Figs. 15(e)-(f) in the approach engagement region while operating the gears under constant load condition.

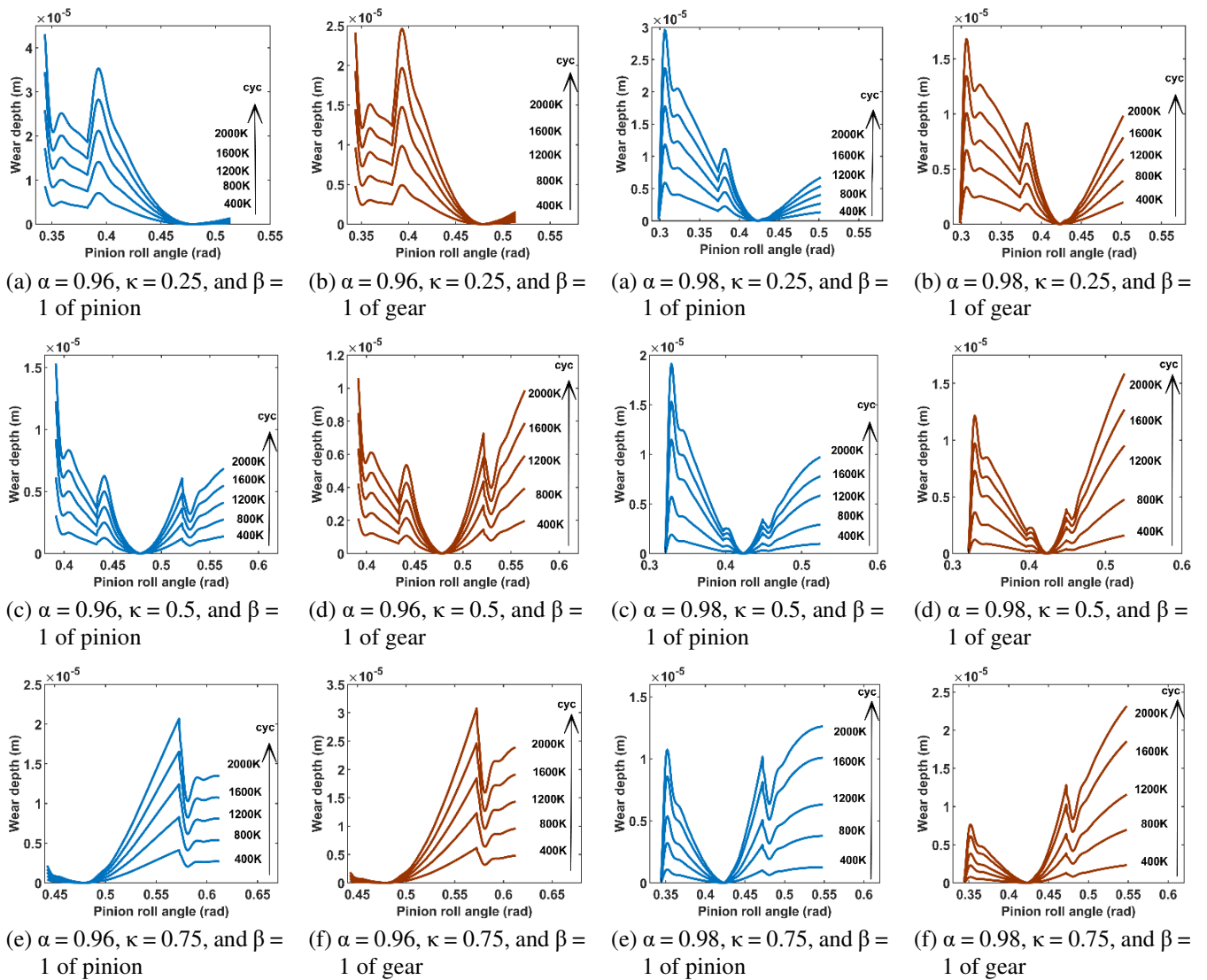


Fig. 14 Wear plots ATS gears $\alpha = 0.96$ for 2×10^6 cycles

Fig. 15 Wear plots ATS gears $\alpha = 0.98$ for 2×10^6 cycles

For tooth-sum alteration factor $\alpha > 1$, the contact transforms from NCR STS to HCR ATS gears, significantly reducing dynamic load factors over ATS gears with lower α values due to reduced unit tooth load and the minimal dimension of the transition zone. Just as in the case of LCR ATS gears, varying the profile shift factor κ alters the mesh zone about the pitch

point in HCR ATS gears. However, unlike the LCR ATS gears, the profile shift factor $\kappa < 0.5$ for any HCR ATS reduces the length of the approach path and increases the recessed path, making the drive recess dominant. The specific sliding decreases at the point of engagement and increases at disengagement for both the pinion and the gear, compared with the ATS HCR gears with profile shift factor $\kappa = 0.5$. Significantly higher specific sliding and very thin oil film in the root region of the gear causes a higher wear rate on the gear than on the pinion (refer to Figs. 16(a)-(b) and Figs. 17(a)-(b)).

The HCR ATS gears with profile shift factor $\kappa = 0.5$ have equal approach-recess action. The root regions of both the pinion and the gear have higher specific sliding and lower oil film thickness than the NCR STS gears under constant load conditions. Consequently, the accumulated wear (refer to Figs. 16(c)-(d) and Figs. 17(c)-(d)) is comparatively greater than NCR STS under constant load conditions. The HCR ATS gears with shift factor $\kappa > 0.5$ have significantly higher specific sliding at the pinion root causing higher wear (refer to Figs. 16(e)-(f) and Figs. 17(e)-(f)) on the pinion than on the gear. Increased specific sliding and reduced oil film thickness due to reduced operating speed cause higher wear rates in HCR ATS gears.

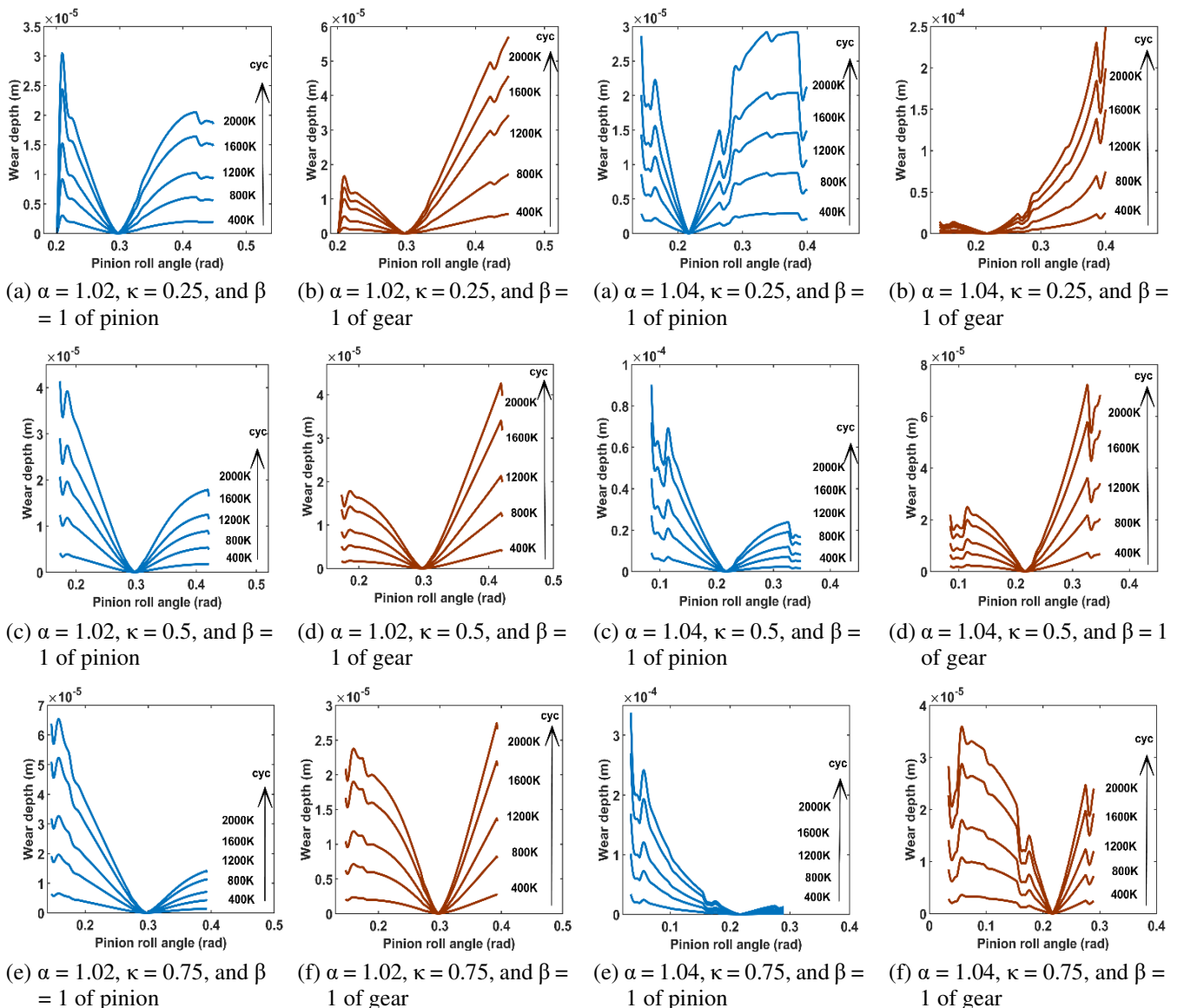


Fig. 16 Wear plots ATS gears $\alpha = 1.02$ for 2×10^6 cycles

Fig. 17 Wear plots ATS gears $\alpha = 1.04$ for 2×10^6 cycles

Tooth tip relief modification is considered one of the well-known ways to reduce dynamic loads and wear in spur gears. To investigate the effectiveness of the tip relief modification in reducing tooth wear in ATS gears, the variations of tip relief for the contact points are integrated into tooth profile deviations as wear (refer to Eq. (45)). The amount of relief is configured based on the design load and the tooth deflection for a test case on LCR ATS with tooth-sum alteration factor $\alpha = 0.96$ and

profile shift factor $\kappa = 0.5$ (refer to Fig. 18). Referring to Figs. 14(c)-(d) and Fig. 19 for comparison of wear on gear and pinion with and without tip relief, the reduction in wear on the latter reflects the reduction in dynamic loads, which is particularly pronounced at the beginning and the end of the mesh.

Different gear ratios of ATS gears of a given tooth-sum also alter the tooth geometry, just like profile shift factors alter the gear geometry since their base circles are different. Superimposing magnitudes of gear ratios and profile shift factors push the start or end of tooth contact very near to the point of tangency to the base circles which may cause extreme sliding operating conditions. Therefore, LCR or HCR ATS gears with $GR > 1$ should be paired with profile shift factors $\kappa < 0.5$ to avoid higher specific sliding. Similarly, LCR or HCR gears with $GR < 1$ should be paired with profile shift factors $\kappa > 0.5$ to avoid extreme operating conditions.

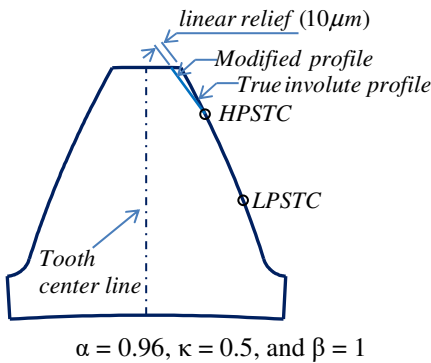
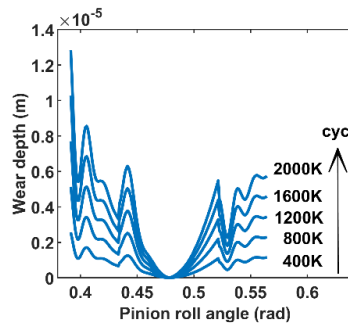
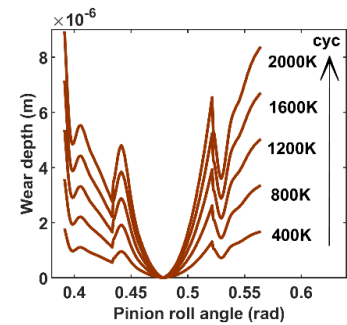


Fig. 18 Tooth with relief modification



(a) $\alpha = 0.96, \kappa = 0.5,$ and $\beta = 1$ of pinion



(b) $\alpha = 0.96, \kappa = 0.5,$ and $\beta = 1$ of gear

Fig. 19 Wear plots for ATS gears with tip relief

11. Conclusions

ATS gear drives are geometry-modified and, kinematically compatible sets of gear pairs capable of operating at a specified center distance. LCR and HCR ATS gear pairs can be obtained by altering the tooth-sum of an NCR STS gear pair with the tooth-sum alteration factor $1 < \alpha < 1$, respectively. Based on the comparative study of the supportive and detrimental effects of tribological aspects affecting surface durability in ATS gears under constant load, the following conclusions are drawn:

- (1) The effects of tooth-sum alteration on surface wear are influenced by meshing parameters such as dynamic load factors, specific sliding, and material properties.
- (2) Specific sliding is an important parameter that is associated with the radius of curvature and speed ratio.
- (3) Zones of higher specific sliding are associated with higher flash temperature, reduced oil viscosity, and increased coefficient of friction.
- (4) LCR ATS gears operating at higher speeds help in the formation of better oil film, and lower specific sliding causes reduced flash temperature that prevents excessive reduction in dynamic viscosity and promotes better oil film thickness. Therefore, the oil film takes up a more significant portion of the load, reducing the coefficient of friction and surface wear, and increasing pitting life.
- (5) Lower operating speeds in HCR ATS and high specific sliding at the start or endpoint of mesh are responsible for higher flash temperatures and reduced dynamic viscosity, which results in very thin oil film formation. Consequently, much of the load is taken up by the asperities causing increased surface wear, higher coefficient of friction, and lower pitting life.
- (6) While operating ATS gears with gear ratios other than unity, it is preferable to use gear ratio and profile shift factor combinations that lower the specific sliding for the reasons mentioned above.

On a concluding note, the study on ATS gears reveals the influence of profile modification resulting from tooth-sum alteration on surface wear and other interdependent parameters. ATS gearing offers flexible design features often unavailable in STS gear design. However, experimental studies on this methodology of gear design are proposed as a scope for future work.

Nomenclature

α	Tooth-sum alteration factor	c	Center distance
β	Center distance alteration factor	c_{eq}	Equivalent Damping coefficient
\ddot{x}_r	Relative acceleration at mesh interface	E	Modulus of elasticity
\dot{x}_r	Relative velocity at mesh interface	F	Total load per unit face width
κ	Profile shift factor	F_t	Total normal load
λ	Mesh stiffness per unit face width	T_f	Flash Temperature
λ_{eq}	Equivalent static mesh stiffness per unit face width	L	Pitting life estimate
μ	Coefficient of friction	f_d	Dynamic load per unit face width
ϕ	Pressure angle	r_a	Radius of the addendum circle
ρ	Radius of curvature	r_b	Radius of the base circle
η	Dynamic viscosity	k_{eq}	Equivalent dynamic Mesh stiffness per unit face width
θ	Roll angle	k_w	Wear Coefficient
ξ	Damping factor	m	Module
ε	Tooth profile error	m_g	Mass per unit face width
σ_{fc}	Contact stress	x	Profile shift coefficient
v_r	Rolling velocity	x_l	Static load factor
V_{ss}	Specific sliding	x_{dl}	Dynamic load factor
X_s	Total profile shift coefficient	x_r	Relative displacement at mesh interface
B	Design Backlash	Y	Tooth topping coefficient
h	Accumulated wear depth	z	Number of teeth
h_c	Oil film thickness	z_s	Tooth-sum of gear pair
$1/\gamma_1$	Load sharing factor for oil film	N	Speed
$1/\gamma_2$	Load sharing factor for surface asperities	f_c	Load per unit face width on surface asperities
E'	Equivalent modulus of elasticity	f_{hy}	Load per unit face width on oil film
b	Face width of the gear and pinion	μ_c	Friction coefficient for asperities
Subscripts		Superscripts	
1, 2	Pinion and gear	a	Altered
s	Standard	r	Reference
w	Working		
x	Any location along the pressure line		
n	Number of cycles		
Abbreviations			
ATS	Tooth-sum altered	NCR	Normal contact ratio
HCR	High contact ratio	rpm	Revolutions per minute
LCR	Low contact ratio	STS	Standard tooth-sum
LPSTC	Low point single tooth contact	HPSTC	High point single tooth contact

Conflicts of Interest

The authors declare no conflict of interest.

References

- [1] H. K. Sachidananda, J. Gonsalvis, and H. R. Prakash, "Experimental Investigation of Fatigue Behavior of Spur Gear in Altered Tooth-Sum Gearing," *Frontiers of Mechanical Engineering*, vol. 7, no. 3, pp. 268-278, September 2012.

- [2] H. K. Sachidananda, K. Raghunandana, and J. Gonsalvis, "Sliding Velocity in Profile-Corrected Gears," *Lubrication Science*, vol. 29, no. 1, pp. 43-58, January 2017.
- [3] A. A. Dsa and J. Gonsalvis, "Enhancing Design Features of Asymmetric Spur Gears Operating on a Specified Center Distance Using Tooth Sum Altered Gear Geometry," *Proceedings of Engineering and Technology Innovation*, vol. 18, pp. 1-14, March 2021.
- [4] H. Moes, "Optimum Similarity Analysis with Applications to Elastohydrodynamic Lubrication," *Wear*, vol. 159, no. 1, pp. 57-66, November 1992.
- [5] J. F. Archard, "Contact and Rubbing of Flat Surfaces," *Journal of Applied Physics*, vol. 24, no. 8, pp. 981-988, August 1953.
- [6] K. L. Johnson, J. A. Greenwood, and S.Y. Poon, "A Simple Theory of Asperity Contact in Elastohydro-Dynamic Lubrication," *Wear*, vol. 19, no. 1, pp. 91-108, January 1972
- [7] J. A. Greenwood and J. B. Williamson, "Contact of Nominally Flat Surfaces," *Proceedings of the Royal Society of London. Series A, Mathematical and Physical Sciences*, vol. 295, no. 1442, pp. 300-319, December 1966.
- [8] E. R. M. Gelinck and D. J. Schipper, "Calculation of Stribeck Curves for Line Contacts," *Tribology International*, vol. 33, no. 3-4, pp. 175-181, April 2000.
- [9] S. Akbarzadeh and M. M. Khonsari, "Performance of Spur Gears Considering Surface Roughness and Shear Thinning Lubricant," *Journal of Tribology*, vol. 130, no. 2, April 2008.
- [10] A. Ebrahimi Serest and S. Akbarzadeh, "Mixed-Elastohydrodynamic Analysis of Helical Gears Using Load-Sharing Concept," *Proceedings of the Institution of Mechanical Engineers, Part J: Journal of Engineering Tribology*, vol. 228, no. 3, pp. 320-331, March 2014.
- [11] M. Kimiaei and S. Akbarzadeh, "Effect of Profile Modification on the Performance of Spur Gears in Isothermal Mixed-EHL Regime Using Load-Sharing Concept," *Proceedings of the Institution of Mechanical Engineers, Part J: Journal of Engineering Tribology*, vol. 233, no. 6, pp. 936-948, June 2019.
- [12] V. Simon, "EHD Lubrication of Different Types of Gears," *Advanced Tribology*, Berlin: Springer, 2009.
- [13] V. Simon, "Elastohydrodynamic Lubrication of Hypoid Gears," *Journal of Mechanical Design*, vol. 103, no. 1, pp. 195-203, January 1981.
- [14] V. Simon, "Improved Mixed Elastohydrodynamic Lubrication of Hypoid Gears by the Optimization of Manufacture Parameters," *Wear*, vol. 438-439, November 2019.
- [15] A. Flodin and S. Andersson, "Simulation of Mild Wear in Spur Gears," *Wear*, vol. 207, no. 1-2, pp. 16-23, June 1997.
- [16] R. Prabhu Sekar and R. Sathishkumar, "Enhancement of Wear Resistance on Normal Contact Ratio Spur Gear Pairs Through Non-Standard Gears," *Wear*, vol. 380-381, pp. 228-239, June 2017.
- [17] F. Karpat and S. Ekwaro-Osire, "Influence of Tip Relief Modification on the Wear of Spur Gears with Asymmetric Teeth," *Tribology Transactions*, vol. 51, no. 5, pp. 581-588, September 2008.
- [18] J. A. Brandão, R. Martins, J. H. Seabra, and M. J. Castro, "An Approach to the Simulation of Concurrent Gear Micropitting and Mild Wear," *Wear*, vol. 324-325, pp. 64-73, February 2015.
- [19] S. Zhang, Z. Sun, and F. Guo, "Investigation on Wear and Contact Fatigue of Involute Modified Gears Under Minimum Quantity Lubrication," *Wear*, vol. 484-485, article no. 204043, November 2021.
- [20] M. Ristivojević, T. Lazovic, and A. Vencl, "Studying the Load Carrying Capacity of Spur Gear Tooth Flanks," *Mechanism and Machine Theory*, vol. 59, pp. 125-137, January 2013.
- [21] H. Ding and A. Kahraman, "Interactions between Nonlinear Spur Gear Dynamics and Surface Wear," *Journal of Sound and Vibration*, vol. 307, no. 3-5, pp. 662-679, November 2007.
- [22] G. M. Maitra, *Handbook of Gear Design*, 2nd ed., Tata McGraw-Hill, 1994.
- [23] J. R. Colbourne, *The Geometry of Involute Gears*, 1st ed., New York: Springer, 1987.
- [24] J. A. Greenwood and J. H. Tripp, "The Contact of Two Nominally Flat Rough Surfaces," *Proceedings of the Institution of Mechanical Engineers*, vol. 185, no. 1, pp. 625-633, June 1970.
- [25] J. H. Kuang and A. Lin, "The Effect of Tooth Wear on the Vibration Spectrum of a Spur Gear Pair," *Journal of Vibration and Acoustics*, vol. 123, no. 3, pp. 311-317, July 2001.
- [26] K. Ichimaru and F. Hirano, "Dynamic Behavior of Heavy-Loaded Spur Gears," *Journal of Engineering for Industry*, vol. 96, no. 2, pp. 373-381, May 1974.
- [27] G. Lundberg and A. Palmgren, "Dynamic Capacity of Rolling Bearings," *Journal of Applied Mechanics*, vol. 16, no. 2, pp. 165-172, June 1949.
- [28] J. J. Coy, D. P. Townsend, and V. Zaretsky, "Analysis of Dynamic Capacity of Low Contact Ratio Spur Gears Using Lundberg-Palmgren Theory," *NASA Technical Report, NASA-TN-D-8029*, August 1975.

